Charm production in pp collisions at 5 and 13 TeV at LHCb

Dominik Müller[*][†]
University of Manchester
E-mail: dominik.muller@cern.ch

The start of the second run of the Large Hadron collider opened a new energy regime in which QCD predictions for charm meson production may be precisely tested. LHCb is uniquely suited to make measurements of production cross-sections in the forward region, as our sensitivity to the gluon parton distribution function in the small-x region can be used to improve the understanding of the proton structure. Having measured charm hadron production cross-sections at multiple proton-proton collision energies, LHCb now has access to cross-section ratios, a more precise class of observables that benefit from cancellation of both experimental and theoretical uncertainties, providing a new sensitive test of the QCD calculations. This paper will give an overview on charm hadron production measurements by LHCb in Run 2 at proton-proton center-of-mass energies of 5 and 13 TeV.

VIII International Workshop On Charm Physics
5-9 September, 2016
Bologna, Italy

---

[*]Speaker.
[†]On behalf of the LHCb collaboration

1. Introduction

Measurements of charm production cross-sections in proton-proton collisions are important tests of perturbative quantum chromodynamics [1, 2, 3], and LHCb can contribute unique measurements in the forward region. With the start of Run 2 of the Large Hadron Collider (LHC) providing pp collisions at a center-of-mass of $\sqrt{s} = 13\,\text{TeV}$, the calculations can be tested in a new energy regime. Furthermore, in preparation for heavy ion collisions, sufficient pp collisions at $\sqrt{s} = 5\,\text{TeV}$ were recorded, allowing cross-sections to be measured at a new energy never studied before.

Differential measurements of J/ψ and D meson production in the forward region test the prediction of quantum chromodynamics to very high values of rapidity, y, and allow to probe a region where the momentum fraction, x, of the initial state partons with respect to the proton momentum reaches values below 10^{-4}. In turn, the differential cross-sections can be used to constrain the low x region gluon parton distribution function (PDF). The sensitivity to the PDF is substantially increased if cross-section measurements at different center-of-mass energies or ratios thereof are considered, which benefit from cancellation of both experimental and theoretical uncertainties. A recent study using all D meson cross-section measurements by LHCb has observed a substantial decrease in the uncertainty on the gluon PDF [4]. Knowledge of the gluon PDF is widely applicable, for example in cosmic neutrino experiments, where atmospheric neutrinos from charm meson decays are the dominant background, probing the same region of x; its precise description is crucial. This paper summarises the cross-section measurements at LHCb of D^0, D^+, D_s^+, and $D^*(2010)^+$ (henceforth denoted as D^{*+}), generally referred to as D in the following, at $\sqrt{s} = 5\,\text{TeV}$ [5] and $\sqrt{s} = 13\,\text{TeV}$ [6], and J/ψ at $\sqrt{s} = 13\,\text{TeV}$ [7]. Measurements of D meson cross-sections have previously been performed by the LHCb experiment at $\sqrt{s} = 7\,\text{TeV}$ [8], and J/ψ cross-sections have been measured at 2.76 TeV [9], 7 TeV [10] and 8 TeV [11].

2. Setup and analysis strategy

The LHCb detector is a single-arm forward spectrometer covering a pseudorapidity range of $2 < \eta < 5$ and is described in detail in Ref. [12, 13]. In Run 2 of the LHC, LHCb employs a new data taking scheme, which the presented analyses exploit: at the beginning of each LHC fill, an alignment and calibration of the detector is performed in real time such that the event reconstruction in the trigger is identical to the offline reconstruction. This enables analyses to be performed directly on the candidates from the trigger which leads to an order of magnitude reduction in the event size, as only the reconstructed candidates need to be saved [14, 15].

The presented analyses reconstruct the final states $J/\psi \to \mu^-\mu^+, D^0 \to K^-\pi^+, D^+ \to K^-\pi^+\pi^+, D_s^+ \to K^-K^+\pi^+$ and $D^* \to D^0\pi^+$ where $D^0 \to K^-\pi^+$. A detailed description of the construction and selection of candidates as well the determination of the reconstruction and selection efficiencies is given in Refs [5, 6, 7]. For all three measurements, the main results are the average double-differential cross-section as a function of the transverse momentum p_T and rapidity y within (p_T, y) bins:

$$\frac{\mathrm{d}^2\sigma_i(M)}{\mathrm{d}p_T\mathrm{d}y} = \frac{1}{\Delta p_{T,i}\Delta y_i} \cdot \frac{N_i(M \to f + \text{c.c.})}{\varepsilon_{i,\text{tot}}(M \to f)\mathcal{B}(M \to f)\mathcal{L}_{\text{int}}}, \tag{2.1}$$

where M refers to any of the studied mesons, $\Delta p_{T,i}$ and Δy_i are the widths of bin i, $N_i(M \to f + \text{c.c.})$ is the measured signal yield for decays of M to the final state f in bin i plus the charge-conjugated decay, $\varepsilon_{i,\text{tot}}(M \to f)$ is the total efficiency for observing the signal decay in bin i, and $\mathscr{B}(M \to f)$ is the branching ratio of the decay to the specific final state, taken from Ref. [16]. The total integrated luminosity, $\mathscr{L}_{\text{int}}$, differs for the different sets of results presented here. The D meson measurements use $5\,\text{pb}^{-1}$ of 13 TeV and $8.6\,\text{pb}^{-1}$ of 5 TeV data while the J/ψ analysis uses $3\,\text{pb}^{-1}$ of 13 TeV data.

3. Results for J/ψ production at 13 TeV

Results for J/ψ production in different J/ψ (p_T, y) bins are presented both for prompt production at the primary vertex (PV) of the pp collision, as well as secondary J/ψ from the decay of heavier, long-lived particles (in the following referred to as from-b). In each (p_T, y) bin, the two contributions are disentangled and separated from combinatorial background events with a likelihood fit to the invariant dimuon mass $m(\mu^+\mu^-)$ and the measured decay time along the beam axis

$$t_z = \frac{(z_{J/\psi} - z_{\text{PV}}) \cdot M_{J/\psi}}{p_z}, \qquad (3.1)$$

where $z_{J/\psi}$ and z_{PV} are the z position of the J/ψ decay vertex and the primary vertex respectively, p_z is the momentum along z of the J/ψ candidate and $M_{J/\psi}$ its invariant mass. As J/ψ decays instantaneously, the measured decay time for prompt J/ψ is compatible with 0 as the decay vertex and the primary vertex are identical while the measured pseudo decay time for J/ψ from-b follows an exponential distribution consistent with the decay of long-lived b-hadrons. The fit is performed in each (p_T, y) bin and an example is given in Fig. 1.
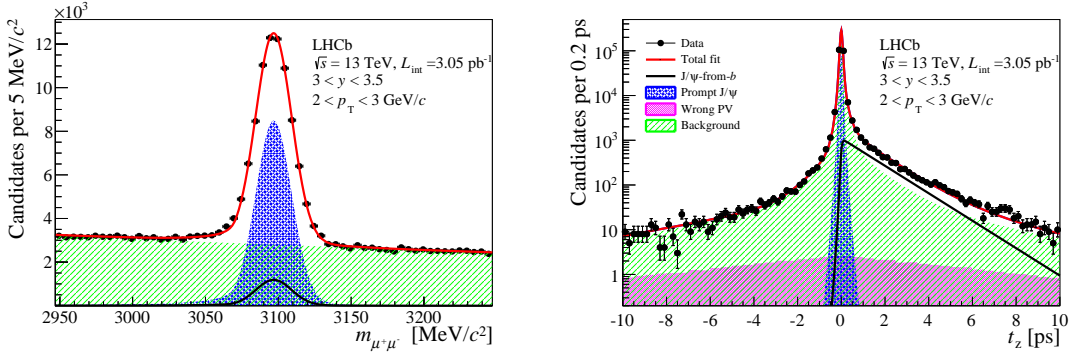

Figure 1: Fits to discriminate between prompt and from-b J/ψ. Projection of two-dimensional fit onto $m(\mu^+\mu^-)$ (left) and t_z (right).

The double differential cross-sections $\mathrm{d}^2\sigma/\mathrm{d}p_T\mathrm{d}y$ for prompt and from-b J/ψ which are given in Fig. 2. From these results, several additional results are derived, most notably single differential cross-sections integrated over y and their ratios between 13 TeV and 8 TeV [11]. Both of these are shown in Fig. 3 for prompt J/ψ and compared to theory predictions obtained from non-relativistic QCD calculations (NRQCD) [17]. Overall, the measured and predicted values are in agreement albeit the measured cross-sections are at the edge of the theory predictions, and the measured
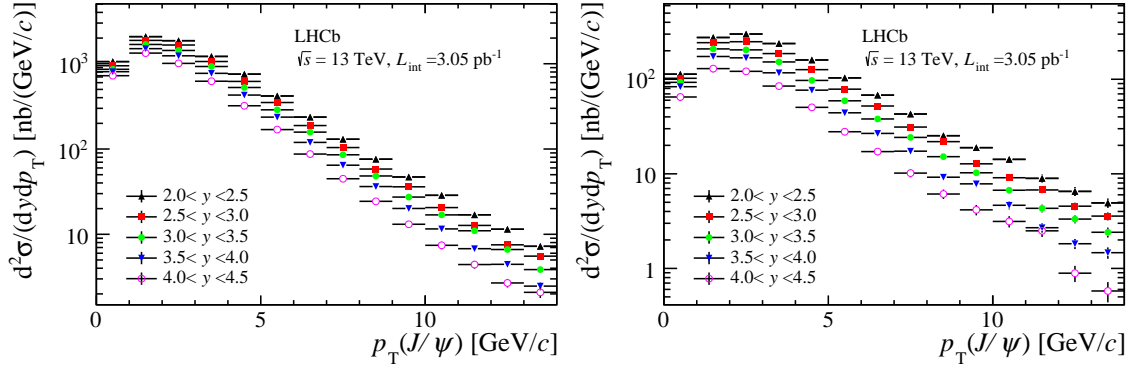
Figure 2: Measured double differential production cross-sections in p_T and y for prompt J/ψ (left) and J/ψ from-b (right).
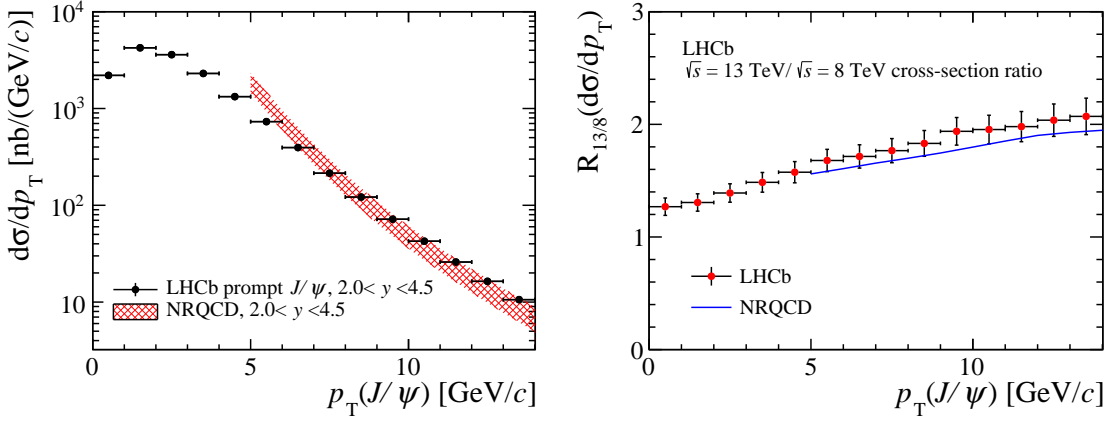

Figure 3: Production cross-sections in bins of p_T and integrated over $2 < y < 4.5$ for prompt J/ψ (left) and their ratios between 13 and 8 TeV (right). Also shown are NRQCD calculations [17].

ratios are found to be consistently above the predictions. Furthermore, integrated cross-sections are computed for prompt and from-b J/ψ in the LHCb acceptance:

$$\sigma_{\text{prompt}} = 15.30 \pm 0.03\,(\text{stat}) \pm 0.86\,(\text{sys})\,\mu\text{b and}$$
$$\sigma_{\text{from-}b} = 2.34 \pm 0.01\,(\text{stat}) \pm 0.13\,(\text{sys})\,\mu\text{b.} \tag{3.2}$$

4. Results for open charm production at 13 TeV and 5 TeV

Measurements of D meson production at $\sqrt{s} = 5$ TeV and $\sqrt{s} = 13$ TeV were made using the same analysis procedure and hence are described together in the following. As was done in the case of the J/ψ measurement, prompt production in the primary vertex and secondary production have to be disentangled, however, the D meson cross-sections are only measured for prompt production while secondary contributions are treated as background. To determine the number of promptly produced charm mesons, a two step fit is performed. The combinatorial background contamination is estimated and constrained from a fit to the invariant mass of the D candidate. Unlike J/ψ's, the D^0, D^+ and D_s^+ mesons do not decay instantaneously, hence t_z cannot be used: both prompt
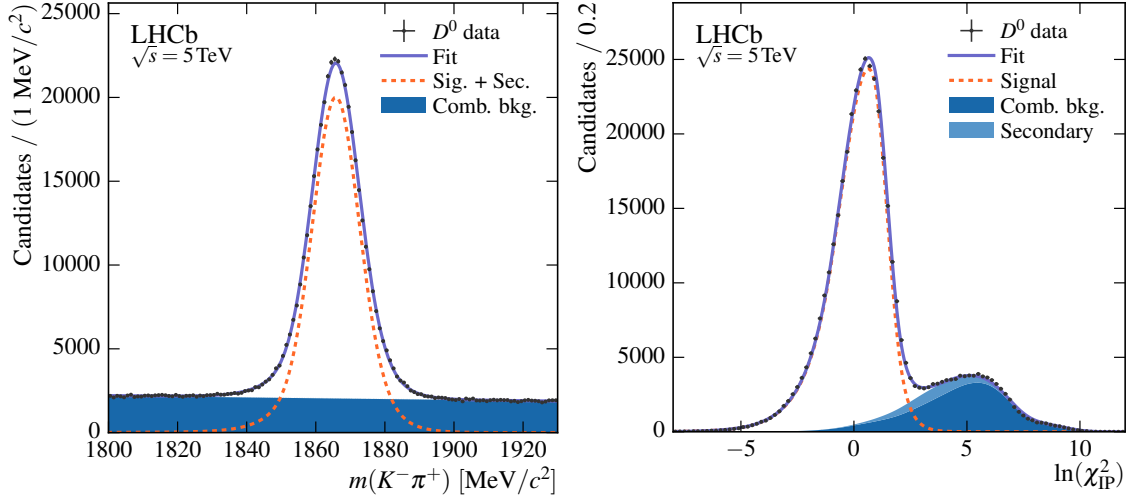
Figure 4: Fits to determine prompt D^0 signal yield. Integrated fit to the invariant mass (left) and integrated fit to $\ln(\chi^2_{IP})$ (right).
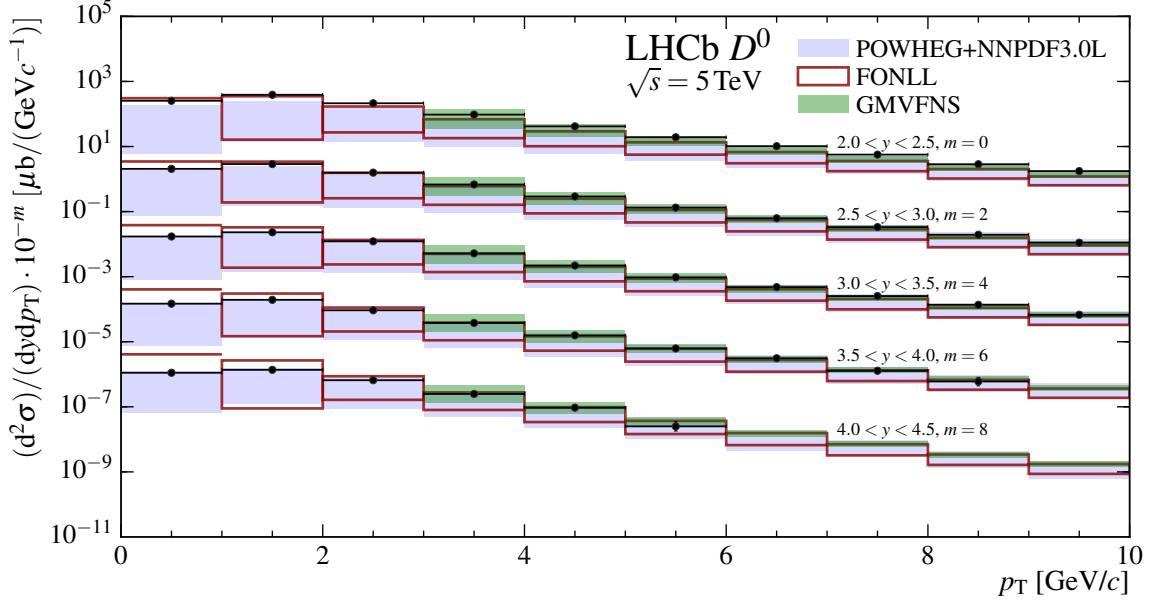

Figure 5: Differential D^0 cross-sections at $\sqrt{s} = 5$ TeV measured in (p_T, y) bins and compared with POWHEG+NNPDF3.0L [1], FONLL [2] and GMVFNS [3] predictions.

and secondary would appear as exponential distributions whose separation in a likelihood fit is challenging. Instead, a second fit to $\ln(\chi^2_{IP})$, where χ^2_{IP} is defined as the difference in χ^2 of the reconstructed PV with and without the D candidate is performed using constraints obtained from the fit to the invariant mass. As for J/ψ, the fit is performed in bins of (p_T, y) and the integrated fit for D^0 in the two variables is shown in Fig. 4. In the following, a limited selection of results is discussed, focussing on D^0 at $\sqrt{s} = 5$ TeV and the remaining results for other D mesons and at $\sqrt{s} = 13$ TeV can be found in the corresponding publications. Fig. 5 shows the measured D^0 cross-

section at $\sqrt{s} = 5$ TeV in (p_T, y) bins, together with three sets of theory predictions [1, 2, 3]. The predictions tend to underestimate the measured cross-sections, although theory and experiment are still in agreement within uncertainties. Fig. 6 shows the cross-section ratios at different pp center-of-mass energies for D^0. The ratios of cross-sections measured at 13 TeV and 7 TeV ratios are generally larger than the predicted values, however the uncertainties on the measured values are large and highly correlated between different bins. This uncertainty is driven by the precision on the 7 TeV measurement. The measurements at 5 TeV are significantly more precise than those at 7 TeV, resulting in a substantial improvement in precision, and a good agreement with predictions is found. Using measured fragmentation fractions $f(c \to D)$ [18], estimates for the total $c\bar{c}$ cross-
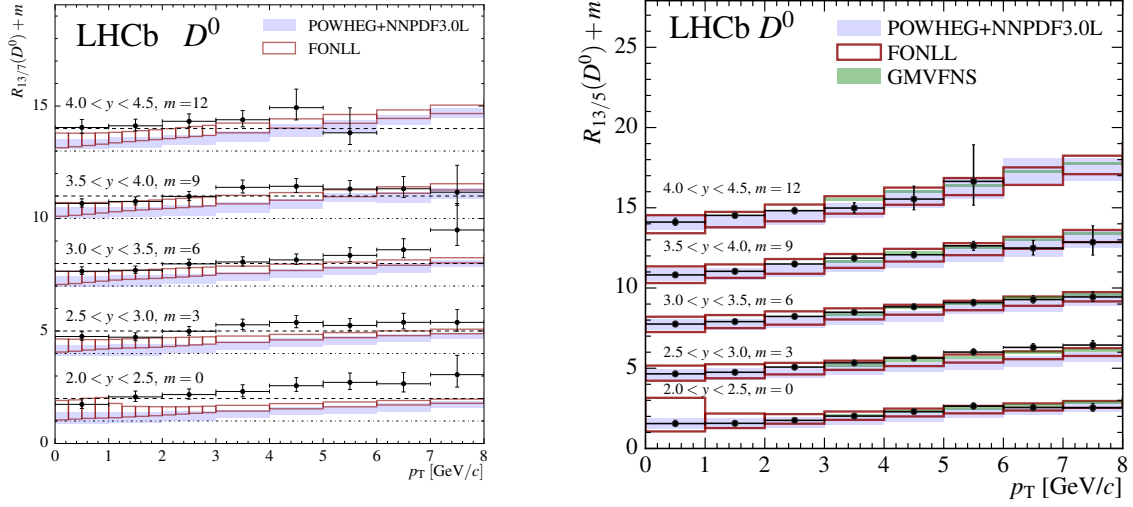

Figure 6: Ratios of 13 TeV to 7 TeV and 5 TeV D^0 cross-sections measurements respectively.

section are computed per meson species and averaged to obtain

$$\sigma(pp \to c\bar{c}X)_{p_\mathrm{T} < 8\,\mathrm{GeV/c},\, 2.0 < y < 4.5, 13\,\mathrm{TeV}} = 2840 \pm 3 \pm 170 \pm 150\,\mu\mathrm{b}, \tag{4.1}$$

$$\sigma(pp \to c\bar{c}X)_{p_\mathrm{T} < 8\,\mathrm{GeV/c},\, 2.0 < y < 4.5,\, 5\,\mathrm{TeV}} = 1395 \pm 5 \pm\ \ 80 \pm\ \ 67\,\mu\mathrm{b}. \tag{4.2}$$

5. Summary

This paper summarises the recent production measurements of charm mesons at LHCb. Measurements of D and J/ψ meson production at 13 TeV have been performed and theoretical predictions underestimate the results. The D meson cross-sections have been measured at 5 TeV and the obtained cross-section ratios with respect to 13 TeV are significantly more precise than those at 7 TeV, and resolve the slight underestimation by the predictions seen.

References

[1] R. Gauld, J. Rojo, L. Rottoli and J. Talbert, *Charm production in the forward region: constraints on the small-x gluon and backgrounds for neutrino astronomy*, *JHEP* **11** (2015) 009, [1506.08025].

[2] M. Cacciari, M. L. Mangano and P. Nason, *Gluon PDF constraints from the ratio of forward heavy-quark production at the LHC at $\sqrt{s} = 7$ and 13 TeV*, *Eur. Phys. J.* **C75** (2015) 610, [1507.06197].

[3] B. Kniehl, G. Kramer, I. Schienbein and H. Spiesberger, *Inclusive charmed-meson production at the CERN LHC*, *Eur.Phys.J.* **C72** (2012) 2082, [1202.0439].

[4] R. Gauld and J. Rojo, *Precision determination of the small-x gluon from charm production at LHCb*, 1610.09373.

[5] LHCʙ collaboration, R. Aaij et al., *Measurements of prompt charm production cross-sections in pp collisions at $\sqrt{s} = 5$ TeV*, 1610.02230 LHCb-PAPER-2016-042, CERN-EP-2016-244, [1610.02230].

[6] LHCʙ collaboration, R. Aaij et al., *Measurements of prompt charm production cross-sections in pp collisions at $\sqrt{s} = 13$ TeV*, *JHEP* **03** (2016) 159 LHCb-PAPER-2015-041, CERN-PH-EP-2015-272, [1510.01707].

[7] LHCʙ collaboration, R. Aaij et al., *Measurement of forward J/ψ production cross-sections in pp collisions at $\sqrt{s} = 13$ TeV* , *JHEP* **10** (2015) 172 LHCb-PAPER-2015-037, CERN-PH-EP-2015-222, [1509.00771].

[8] LHCʙ collaboration, R. Aaij et al., *Prompt charm production in pp collisions at $\sqrt{s} = 7$ TeV* , *Nucl. Phys.* **B871** (2013) 1 LHCb-PAPER-2012-041, CERN-PH-EP-2013-009, [1302.2864].

[9] LHCʙ collaboration, R. Aaij et al., *Measurement of J/ψ production in pp collisions at $\sqrt{s} = 2.76$ TeV* , *JHEP* **02** (2013) 041 CERN-PH-EP-2012-349, LHCb-PAPER-2012-039, [1212.1045].

[10] LHCʙ collaboration, R. Aaij et al., *Measurement of J/ψ production in pp collisions at $\sqrt{s} = 7$ TeV*, *Eur. Phys. J.* **C71** (2011) 1645 CERN-PH-EP-2011-018, LHCb-PAPER-2011-003, [1103.0423].

[11] LHCʙ collaboration, R. Aaij et al., *Production of J/ψ and Υ mesons in pp collisions at $\sqrt{s} = 8$ TeV* , *JHEP* **06** (2013) 064 CERN-PH-EP-2013-071, LHCb-PAPER-2013-016, [1304.6977].

[12] LHCʙ collaboration, A. A. Alves Jr. et al., *The LHCb detector at the LHC*, *JINST* **3** (2008) S08005.

[13] LHCʙ collaboration, R. Aaij et al., *LHCb detector performance*, *Int. J. Mod. Phys.* **A30** (2015) 1530022, [1412.6352].

[14] R. Aaij et al., *The LHCb trigger and its performance in 2011*, *JINST* **8** (2013) P04022, [1211.3055].

[15] R. Aaij et al., *Tesla: An application for real-time data analysis in High Energy Physics*, 1604.05596.

[16] Pᴀʀᴛɪᴄʟᴇ Dᴀᴛᴀ Gʀᴏᴜᴘ collaboration, K. A. Olive et al., *Review of particle physics*, *Chin. Phys.* **C38** (2014) 090001.

[17] H.-S. Shao, H. Han, Y.-Q. Ma, C. Meng, Y.-J. Zhang and K.-T. Chao, *Yields and polarizations of prompt j/ψ and ψ(2s) production in hadronic collisions*, *JHEP* **2015** (2015) 1–18.

[18] Pᴀʀᴛɪᴄʟᴇ Dᴀᴛᴀ Gʀᴏᴜᴘ collaboration, C. Amsler et al., *Fragmentation functions in e^+e^- annihilation and lepton-nucleon DIS,* in *Review of particle physics*, *Phys. Lett.* **B667** (2008) 1.

PoS(CHARM2016)061